Atmos. Chem. Phys. Discuss., 6, 2765–2807, 2006
www.atmos-chem-phys-discuss.net/6/2765/2006/

Atmospheric Chemistry and Physics Discussions

Measuring atmospheric CO_2 from space using Full Spectral Initiation (FSI) WFM-DOAS

M. P. Barkley[1], U. Friedß[1,*], and P. S. Monks[2]

[1]EOS, Space Research Centre, Department of Physics & Astronomy, University of Leicester, Leicester, LE1 7RH, UK
[2]Department of Chemistry, University of Leicester, Leicester, LE1 7RH, UK
[*]now at: Institute of Environmental Physics, Heidelberg, Germany

Received: 6 December 2005 – Accepted: 10 February 2006 – Published: 10 April 2006

Correspondence to: P. S. Monks (psm7@le.ac.uk)

Abstract

Satellite measurements of atmospheric CO_2 concentrations are a rapidly evolving area of scientific research which can help reduce the uncertainties in the global carbon cycle fluxes and provide insight into surface sources and sinks. One of the emerging CO_2 measurement techniques is a relatively new retrieval algorithm called Weighting Function Modified Differential Optical Absorption Spectroscopy (WFM-DOAS) that has been developed by Buchwitz et al. (2000). This algorithm is designed to measure the total columns of CO_2 (and other greenhouse gases) through the application to spectral measurements in the near infrared (NIR), made by the SCIAMACHY instrument on-board ENVISAT. The algorithm itself is based on fitting the logarithm of a model reference spectrum and its derivatives to the logarithm of the ratio of a measured nadir radiance and solar irradiance spectrum. In this work, a detailed error assessment of this technique has been conducted and it has been found necessary to include suitable a priori information within the retrieval in order to minimize the errors on the retrieved CO_2 columns. Hence, a new CO_2 retrieval algorithm called Full Spectral Initiation (FSI) WFM-DOAS has been developed which generates a reference spectrum for each individual SCIAMACHY observation using the known properties of the atmosphere and surface at the time of the measurement. Initial retrievals over Siberia during the summer of 2003 show that the measured CO_2 columns are not biased from the input a priori data and that whilst the monthly averaged CO_2 distributions contain a high degree of variability, they also contain significant spatial features.

1 Introduction

The carbon cycle is one of the most important physical systems on the Earth and its response to increased levels of atmospheric CO_2 and to global warming is one of the factors that will shape the future climate. In the natural cycle, carbon is continually transported between the atmosphere, ocean and terrestrial biosphere through fluxes

that are of order of tens of billion tons per year (Intergovernmental Panel on Climate Change, 2001). Over the last 200 years humans have perturbed this natural cycle by adding comparatively small, but nevertheless significant amounts of carbon into the atmosphere through the burning of fossil fuels, deforestation and by the industrial production of cement, lime and ammonia. Consequently during this period the concentration of atmospheric CO_2 has risen by about 30%, soaring from 270 to 370 ppmv (parts per million by volume). Only approximately half of the total anthropogenic carbon emitted into the atmosphere actually remains there, the rest being absorbed by the oceans and terrestrial biosphere. Carbon that eventually reaches the deep oceans is considered to be removed from the climate system for several hundred years whereas that sequestered by the biosphere may subsequently be released back to the atmosphere over much shorter timescales. The variability and efficiency of the oceanic and terrestrial fluxes will therefore be critical in determining future atmospheric CO_2 levels.

Currently these fluxes are estimated using inverse methods that employ transport models coupled with surface measurements of the atmospheric concentration (e.g. Rödenbeck et al., 2003). However, such models are hampered firstly by the accuracy of the meteorological fields that drive them and secondly by the sparseness and inhomogeneous geographical distribution of the approximately one hundred CO_2 measurements sites that provide the observational constraints (GLOBALVIEW-CO_2, 2005). Although this approach firmly suggests a Northern Hemisphere terrestrial sink (Tans et al., 1990; Ciais et al., 1995), it is somewhat limited as it cannot fully resolve the North American and Eurasian components nor can it determine the extent of the fluxes in the Southern Oceans (Gurney et al., 2002). Knowledge of such regional scale fluxes and the processes that control them can be vastly improved through sampling the atmosphere more comprehensively. The optimal way to achieve this is to make observations from space.

However, this is a challenging observational problem as CO_2 is considered to be well mixed within the atmosphere owing to its long lifetime. As it is chemically inert, its distribution is influenced by transport processes and through the spatial and temporal

variability of both natural and anthropogenic surface fluxes. Seasonal and geographical trends and gradients are evident, not only at the surface but also within the free troposphere and lower stratosphere, typically with an observed variability of about 1–20 ppmv (Nakazawa et al., 1991, 1992; Conway et al., 1994; Anderson et al., 1996; Nakazawa et al., 1997; Vay et al., 1999; Kuck et al., 2000; Levin et al., 2002; Matsueda et al., 2002; Sidorov et al., 2002). That aside, total columns of CO_2 exhibit about only half the variability at the surface with the diurnal fluctuations rarely exceeding 1 ppmv (Olsen and Randerson, 2004). Such small fluctuations in the CO_2 concentration will only therefore produce correspondingly small changes in radiance at the top of the atmosphere (Mao and Kawa, 2004). Since carbon dioxide is a strong absorber, any space-borne sensor will need to detect such minor responses against what is a dominant background signal. The detection of small radiance changes against this strong background requires measurements to be made at high precision, challenging the instrumental limits of the current suite of available sensors. If satellite observations are to improve over the existing ground network, monthly averaged column data at a precision of 1% (2.5 ppmv) or better, for an $8^{\circ} \times 10^{\circ}$ footprint are needed (Rayner and O'Brien, 2001).

Over the last several years various sensitivity analyses have been undertaken to assess if this 1% precision is attainable by satellite instruments. These have mostly focussed on the retrieval of total columns from either the near infrared (NIR) using differential absorption optical spectroscopy (DOAS) (O'Brien and Rayner, 2002; Dufour and Bréon, 2003; Kuang et al., 2002) or from the close examination of the CO_2 emission bands in the thermal infrared (Chédin et al., 2003). Light in the thermal IR originates from the mid-troposphere in contrast to the reflected sunlight of the near infrared. Thus the near surface sensitivity of the NIR makes it the ideal spectral region for observing surface fluxes (even though the absorption bands at 4 μm and 15 μm are much stronger). In addition the NIR is less sensitive to temperature and water vapour.

Since the launch of the SCIAMACHY instrument on-board the European ENVISAT satellite, there is now an ability to measure total columns of CO_2 and other greenhouse

gases from spectral measurements in the NIR. Observations of CO_2 (Houweling et al., 2005), carbon monoxide (CO) (Frankenberg et al., 2005b; Buchwitz et al., 2004) and methane (CH_4) (Frankenberg et al., 2005a) have been performed. From these studies, a global CO_2 data set for 2003 has been prepared by Buchwitz et al. (2005), using a relatively new retrieval algorithm called "Weighting Function Modified Differential Optical Absorption Spectroscopy" (WFM-DOAS). In this paper the SCIAMACHY/WFM-DOAS approach is used but developed further with the aim of increasing the precision and accuracy of space-borne CO_2 retrieval. An initial assessment of this algorithm's sensitivity is given, highlighting the necessity for the inclusion of suitable a priori information within the retrieval in order to constrain the errors on the retrieved CO_2 columns. Furthermore, a new CO_2 retrieval algorithm called "Full Spectral Initiation" (FSI) WFM-DOAS is introduced that is biased towards the known properties of the atmosphere and surface at the time of the SCIAMACHY observation.

The structure of this paper is as follows. In Sect. 2 the SCIAMACHY instrument is briefly described before the WFM-DOAS retrieval technique and an error assessment of its performance is discussed in Sect. 3. In Sect. 4 the FSI WFM-DOAS retrieval algorithm is introduced with some initial results shown in Sect. 5. The paper finishes with a summary in Sect. 6.

2 The SCIAMACHY instrument

The SCanning Imaging Absoprtion spectroMeter for Atmospheric CHartographY (SCIAMACHY) is a passive hyper-spectral UV-VIS-NIR grating spectrometer (Bovensmann et al., 1999). It was launched onboard the ENVISAT satellite in March 2002 into a polar sun-synchronous orbit, crossing the Equator on its descending node (i.e. southwards) at 10.00 a.m. local time. The instrument covers the spectral range 240–2380 nm, non-continuously, in eight separate channels, with a moderate resolution of 0.2–1.4 nm. From its orbit, SCIAMACHY can observe the Earth from three distinct viewing geometries nadir, limb and lunar/solar occultation, with the majority of the or-

bit consisting of measurements in an alternating limb and nadir sequence. The total columns of CO_2 are derived from nadir observations in the NIR, focussing on a small wavelength window within channel six, centered on the CO_2 band at 1.57 μm. The radiation in this wavelength interval consists of solar energy either reflected from the surface or scattered from the atmosphere. In nadir mode, the atmosphere directly below the sensor is viewed producing retrievals with good spatial but poor vertical resolution. A characteristic set of observations consists of the nadir mirror scanning across track for 4 s followed by a fast 1 s back-scan. This is repeated for either 65 or 80 s according to the orbital region. The ground swath viewed has a fixed dimensions of 960×30 km^2, (across × along track). For channel 6, the nominal size of each pixel within the swath is 60×30 km^2, corresponding to an integration time of 0.25 s. Global coverage is achieved at the Equator within 6 days.

3 Assessment of the WFM-DOAS retrieval algorithm

3.1 WFM-DOAS

The WFM-DOAS algorithm (Buchwitz et al., 2000; Buchwitz and Burrows, 2004) defined in Eq. (1), is based on a linear least squares fit of the logarithm of a model reference spectrum I_i^{ref} and its derivatives, plus a quadratic polynomial P_i, to the logarithm of the measured sun normalized intensity I_i^{meas}.

$$\left\| ln I_i^{\mathrm{meas}}(\mathbf{V}^t) - \left[\ln I_i^{\mathrm{ref}}(\bar{\mathbf{V}}) + \frac{\partial \ln I_i^{\mathrm{ref}}}{\partial \bar{V}_{\mathrm{CO_2}}} \cdot (\hat{V}_{\mathrm{CO_2}} - \bar{V}_{\mathrm{CO_2}}) \right. \right.$$

$$\left. \left. + \frac{\partial \ln I_i^{\mathrm{ref}}}{\partial \bar{V}_{\mathrm{H_2O}}} \cdot (\hat{V}_{\mathrm{H_2O}} - \bar{V}_{\mathrm{H_2O}}) + \frac{\partial \ln I_i^{\mathrm{ref}}}{\partial \bar{V}_{\mathrm{Temp}}} \cdot (\hat{V}_{\mathrm{Temp}} - \bar{V}_{\mathrm{Temp}}) \right.$$

ACPD
6, 2765–2807, 2006

$$+ P_j(a_m)\Big]\Big\|^2 \equiv \|\mathrm{RES}_i\|^2 \rightarrow \min \text{ w.r.t } \hat{V}_j \,\&\, a_m \quad (1)$$

The subscript i refers to each detector pixel of wavelength λ_i and the true, model and retrieved vertical columns are represented by $\mathbf{V}^t=(V^t_{CO_2}, V^t_{H_2O}, V^t_{Temp})$, $\bar{\mathbf{V}}=(\bar{V}_{CO_2}, \bar{V}_{H_2O}, \bar{V}_{Temp})$ and $\hat{V}_j$ respectively (where subscript j refers to the variables CO_2, H_2O and temperature). Here V_{Temp} is not a vertical column as such, but rather a scaling factor applied to the vertical temperature profile. Each derivative (or column weighting function) represents the change in radiance as a function of a relative scaling of the corresponding trace gas or temperature profile. Effectively the column weighting functions are replacing the absorption cross sections found in normal DOAS methods. In order to retrieve carbon dioxide derivatives for CO_2, H_2O and (optionally) temperature are required. In the case of the temperature derivative, the term $(\hat{V}_{Temp}-\bar{V}_{Temp})$ represents a uniform shift in the entire temperature profile. The fit parameters are the trace gas columns $\hat{V}_{CO_2}$ and $\hat{V}_{H_2O}$, the temperature scaling factor $\hat{V}_{Temp}$ and the polynomial coefficients a_m.

Although an initial error analysis was performed by Buchwitz and Burrows (2004) a more thorough study has been conducted, and summarized here, to assess possible biases and retrieval errors. It is not the aim of this paper to repeat their efforts but rather to highlight the most important sources of inaccuracy. To achieve this synthetic measurements for a given atmospheric state and instrument set-up were generated using the radiative transfer model SCIATRAN (Rozanov et al., 2002). Simulated retrievals were then performed using a standard reference spectrum, so that in each case the retrieved CO_2 column could be compared to its true value. This reference spectrum was constructed using the US Standard atmosphere (McClatchey et al., 1972) together with a default aerosol scenario (unless indicated otherwise). The CO_2 profile was scaled to coincide with its current concentration of 370 ppmv. Aerosols were parameterized by the LOWTRAN scheme (Kneizys et al., 1986, 1996) the default setting being a spring/summer season with maritime aerosols in the boundary layer (visibility

23 km and humidity 80%). Background tropospheric and stratospheric aerosol conditions were assumed in conjunction with a normal mesospheric loading. Both the solar zenith and the relative azimuth angles (both 45°) and the albedo at 0.2 were kept constant throughout the studies (unless indicated). Each spectrum was created on a high resolution wavelength grid and then convolved with a Gaussian slit function of 1.4 nm (FWHM) before being interpolated onto the SCIAMACHY wavelength grid. The fitting window used throughout this sensitivity analysis was confined to the wavelength region 1561.03–1585.39 nm (see Sect. 4) which, besides the CO_2 band, contains some weak water vapour absorption lines. Weighting functions for CO_2 and H_2O, together with the quadratic polynomial were always included in the WFM-DOAS fit. However for each scenario the simulated retrieval was performed both with and without the temperature weighting function, thus allowing its contribution to be assessed. In this sensitivity study, the relative column error E_{rel}, that is the percentage difference between the retrieved CO_2 column $\bar{V}^{\text{ret}}$ and the actual column $\bar{V}^{\text{actual}}$, is used to gauge the accuracy of each simulated retrieval (Eq. 2).

$$E_{\text{rel}} = \frac{\bar{V}^{\text{ret}} - \bar{V}^{\text{actual}}}{\bar{V}^{\text{actual}}} \times 100\% \tag{2}$$

3.2 Sensitivity to CO_2 vertical profile

The CO_2 profile associated with the US Standard atmosphere has a uniform volume mixing ratio of 370 ppmv, up to an altitude of 80 km. For the tropical regions, where vertical mixing is rapid, this is a fair representation. For higher latitudes however, the shape of the profile is more strongly influenced by dynamics and biospheric activity thus varying seasonally (Anderson et al., 1996; Nakazawa et al., 1997). To ascertain the sensitivity of the algorithm to the vertical CO_2 distribution, simulated retrievals were performed using spectra generated from profiles more representative of the global latitudinal and seasonal CO_2 distribution (illustrated in Fig. 1). These were taken from a new climatology prepared by J. Remedios (University of Leicester, private communica-

tion, 2005). In each simulation the CO_2 profile was interpolated onto the US Standard pressure scale and used in conjunction with the US Standard water vapour profile.

The results from these simulations show that the shape of the CO_2 profile used to create the model reference spectra is important (Fig. 2). Using a uniform CO_2 profile tends to lead to an over-estimation of the true CO_2 concentration irrespective if the temperature weighting function is fitted. The relative error in the retrieved column varies throughout the year and is most pronounced in the Northern Hemisphere where it follows the seasonal cycle, peaking in the month of April at ~0.5%. In the Southern Hemisphere, where the CO_2 distribution is dominated by inter-hemispheric mixing, this seasonal variation is not observed and the error is smaller, typically less than 0.2%. Failure to use realistic a priori CO_2 vertical profiles within the WFM-DOAS algorithm will therefore introduce time-dependent biases.

3.3 Sensitivity to temperature and water vapour profiles

The U.S. standard atmosphere, used to generate the baseline scenario, represents an average climatology whereas the real environment itself is obviously more varied especially between the distinct latitude bands of the tropics, mid latitudes and sub-polar regions. Water vapour and temperature profiles representative of these areas (McClatchey et al., 1972) were consequently used to produce a series of simulated measurements in a similar manner to Buchwitz and Burrows (2004). However, to create a much wider range of atmospheric states both the CO_2 and H_2O trace gas profiles were also multiplied by constant factors (where the CO_2 profile here, refers to that of the US Standard atmosphere). In an addition to this, a further set of simulated measurements was created from 16 ECMWF (un-scaled) temperature and water vapour profiles selected from the months of January and July 2003. These were chosen on the basis of being strongly deviant from the U.S. standard atmosphere (see Fig. 3).

These simulations reveal that the accuracy of the retrieved CO_2 column is highly dependent on the inclusion of the temperature weighting function within the WFM-DOAS fit. If the temperature derivative is included, then in the case of the regional profiles

(Table 1) the errors are less than 1% even when there is coincidental uniform scaling of the CO_2 profile. When more realistic ECMWF profiles are used to generate the synthetic measurements, these errors are larger typically <1.5%, without any additional scaling of the CO_2 concentration (Table 2). Using a climatological mean profile to produce the baseline spectrum is hence inadequate, suggesting that a priori knowledge of the temperature and water vapour profiles is needed when applying WFM-DOAS to real SCIAMACHY spectra. Even if the reference spectra are created from assimilated atmospheric profiles, the temperature derivative must be always included within the retrieval to limit this source of error. This is also clearly demonstrated by examining the retrieval around the temperature linearization point. To accomplish this, a third set of synthetic measurements was created by applying small temperature shifts of 1 K to the US Standard atmosphere (up to a maximum of ±10 K). The subsequent retrievals reveal that not fitting the temperature derivative can produce a relative error in the CO_2 column of as much as ±1.3% for a uniform ±5 K difference between the true and reference temperature profiles (Fig. 4). If the temperature weighting function is fitted, this error is kept to less than 0.1%.

3.4 Sensitivity to CO_2 profile and atmospheric profile

Sections 3.2 and 3.3 have shown that the sufficient knowledge CO_2, temperature and water vapour profiles is necessary to produce accurate retrievals. It is possible to investigate the combined effect of using alternative CO_2 and atmospheric profiles by interpolating the CO_2 profiles, from the new climatology (Sect. 3.2), onto the appropriate tropical, mid-latitude and sub-arctic regional profiles. The consequent simulations show that relative errors in the retrieved column in the order 0.5% can be produced (Fig. 5). Unlike the analysis in Sect. 3.2, the temperature derivative has a much bigger effect. Whilst in the tropics these errors are almost constant throughout the year, at mid and high latitudes they vary seasonally. During the winter months the mid-latitude columns are systematically overestimated by about 0.75% as compared to the summer where they are underestimated by an average of 0.13%. These biases will increase if

the CO_2 profiles are interpolated onto the more lifelike ECMWF profiles. Retrievals performed without using realistic CO_2 profiles *and* realistic temperature and water-vapour profiles and will therefore result in the terrestrial biosphere fluxes in the Northern mid-latitudes being overestimated. Since the natural variability of atmospheric CO_2 total columns is only about 3% these errors are not negligible.

3.5 Sensitivity to the surface elevation and pressure

The surface pressure must be carefully considered in any CO_2 retrieval algorithm. Firstly, because gradients in the atmospheric CO_2 concentration created by variations in the surface topography and low altitude weather systems can often mask those produced by surface fluxes (Kawa et al., 2004) and secondly because the measurement is sensitive to pressure, owing to the broadening of absorption lines (Frankenberg et al., 2005c). The error in the retrieved column as a function of the surface pressure was investigated by varying the surface elevation within the SCIATRAN model. Inspection of the results (Fig. 6) shows that the retrieved column is systematically under-estimated when the surface elevation is increased relative to that used in the reference scenario. The magnitude of this error is approximately −0.31% per 50 m increase in surface elevation, when the temperature weighting function is not fitted, as opposed to approximately −0.34% per 50 m when it is included.

3.6 Sensitivity to the surface albedo

The Earths surface reflectance within the near infra-red can vary from as little as 0.001 over the oceans to as much 0.4 over the desert (Dufour and Bréon, 2003). This affects not only the overall amount of solar radiation reflected back to space (and subsequently the signal to noise ratio of SCIAMACHY measurements) but also the relative depth of CO_2 and H_2O absorption lines by influencing the path-length traveled by the photons (Buchwitz and Burrows, 2004). To gauge this effect, the column error as a function of the surface reflectance was examined using a reference spectrum produced with

an albedo of 0.1 (so as to be consistent with current implementations of WFM-DOAS (Buchwitz et al., 2005). Variations in the surface albedo alone, from 0.05 to 0.4, can cause an error in the retrieved column of up to 2% (Fig. 7). The errors increase further still at very low albedos. Employing a fixed albedo within the algorithm, will thus introduce what are essentially unnecessary errors.

3.7 Sensitivity to aerosols

Retrievals of CO_2 in the near infra-red are affected by the presence of aerosols (Dufour and Bréon, 2003). For example, systematic errors caused by Saharan dust, have already been clearly identified in CO_2 columns retrieved from SCIAMACHY (Houweling et al., 2005). Aerosols can both scatter and absorb light depending on their composition. Aerosol scattering mainly shortens the photon path-length leading to an underestimation of the CO_2 column. To determine their influence on WFM-DOAS, a set of scenarios were created based on the aerosol types defined by Hess et al. (1998) using a parameterization developed by Hoogen (1995). Aerosol extinction profiles were taken (and adapted) from the LOWTRAN library (Kneizys et al., 1996). These aerosols were confined to the boundary layer with background tropospheric and stratospheric conditions assumed. Retrievals simulated using the default scenario show that the errors are lower than 2%, except in extreme cases, and that they increase if the temperature derivative is included within the fit (Table 3). The background marine conditions associated with the reference spectrum however produces biases when applied to contrasting conditions, for example with urban, biomass burning and desert scenarios. This may have repercussions for trying to estimate CO_2 emissions over large urban areas or regions affected by wild fires. However, the inclusion of some background aerosols within the reference spectrum is clearly better than retrievals performed on the basis of an aerosol free atmosphere.

3.8 Fitting of height resolved weighting functions

The non-linearity of DOAS fitting within the near infra-red spectral region, owing to strong absorbers and the effects of pressure broadening, was clearly identified by Frankenberg et al. (2005c). To account for this difficulty, scaling factors for different height layers were used within the IMAP retrieval algorithms state vector. To determine whether the sensitivity of WFM-DOAS could be improved by using this approach, the trace gas columns and associated weighting functions of the reference spectrum, were grouped into three individual height layers: 0–3 km, 3–12 km and 12 km to top of the atmosphere (each column derivative being simply the sum of a set of height resolved weighting functions). The simulated retrievals were then repeated and the resulting errors compared to those obtained using the original column derivatives. In contrast to the findings of Frankenberg et al. (2005c) there was little evidence of increased sensitivity from using this method.

4 Full Spectral Initiation (FSI) WFM-DOAS

The WFM-DOAS algorithm is able to detect changes in the atmospheric CO_2 concentration. However if the CO_2 column is retrieved using a reference spectrum created from a scenario that differs from the true atmospheric state, significant errors could be introduced. As demonstrated, factors which affect the calculated model spectrum are the surface albedo, surface pressure, aerosols and the vertical profiles of CO_2, water vapour and temperature. When varied alone each of these parameters creates an error in the column of typically less than about 2%. However, in the real atmosphere none are known exactly, thus the errors propagate accordingly and are especially significant when considering the high precision measurements that are needed to observe the small gradients associated with atmospheric CO_2. To reduce these errors a reference spectrum that is very close to the real measurement must be used, i.e. as much "a priori" information must be included in the retrieval as possible. It is on this basis that

ACPD
6, 2765–2807, 2006

a new retrieval algorithm called Full Spectral Initiation or (FSI)-WFM-DOAS has been developed. In FSI, a reference spectrum is generated for every single SCIACMACHY measurement to obtain the best linearization point for the retrieval. Subsequent iterations are not performed, in order to limit the computational time. Were this not an issue, then the retrieved parameters would be fed back into the algorithm iteratively. To calculate the best possible reference spectrum all the known or rather estimated properties of the atmosphere and surface at the time of the observation, serve as input for the radiative transfer model. Once the sun-normalised radiance is obtained, a WFM-DOAS fit is then performed and the vertical column retrieved.

The FSI algorithm is applied to calibrated radiances using the fitting window 1561.03–1585.39 nm. This region was chosen in order to minimize interference from water vapour and not to extend into channel 6+, where the Indium Gallium Arsenide (InGaAs) detectors were doped with higher amounts of Indium leading to different behavioural characteristics (Lichtenberg et al., 2005). The number of fitting points within this micro-window is usually thirty-two, with each detector pixel spanning a wavelength interval of 0.7 nm. At this resolution, SCIAMACHY is close to under-sampling the CO_2 band. This spectral interval is also advantageous in that, unlike channels 7 and 8, it is unaffected by orbital variations of the dark current and the build up of ice-layers on the detectors (as discussed by Gloudemans et al., 2005). It is also stable with regard to so called "dead and bad pixels" created by thermal and radiation degradation (Kleipool, 2004). The SCIAMACHY pixel mask, however is checked and if necessary, updated for each orbit using the standard deviations of the dark current, as proposed by Frankenberg et al. (2005b). Detector pixels are also discarded if erroneous spikes occur in the measured radiance. All measurements have been corrected for non-linear effects (Kleipool, 2003b) and the dark current (Kleipool, 2003a). The FSI algorithm also uses a solar reference spectrum with improved calibration, provided to the SCIAMACHY community by ESA, courtesy of Johannes Frerick (ESA, ESTEC), in preference to that in the official L1C product. An optimised systematic shift, based on the inspection of the fit residuals, of 0.15 nm is applied to the observed spectra to align it to the synthetic

radiances calculated by SCIATRAN. To improve the quality of the FSI spectral fits, the latest version of the HITRAN molecular spectroscopic database has been implemented in the radiative transfer model (Rothman et al., 2005).

Each SCIAMACHY observation has an associated reference spectrum created from several sources of atmospheric and surface data. The CO_2 profile is selected from the new climatology (Sect. 3.2) and is chosen according to the time of the observation and the latitude band in which the ground pixel falls. To obtain the closest atmospheric state to the observation temperature, pressure and water vapour profiles, derived from operational 6 hourly ECMWF data ($1.125^\circ \times 1.125^\circ$ grid), are interpolated onto the local overpass time and centre of the of the SCIAMACHY pixel. To determine the linearization point for the surface albedo, a look-up table of mean radiances, for the defined fitting window, has been generated as a function of both the surface reflectance and solar zenith angle. From using the mean radiance of the SCIAMACHY observation and the solar zenith angle at the corresponding time, it is possible to infer an approximate value for the albedo. To account for aerosols, three scenarios are incorporated into the retrieval algorithm. Maritime and rural scenarios are implemented over the oceans and land respectively. In both cases, the boundary layer visibility is 23 km. If a major city occurs within the SCIAMACHY footprint then an urban scenario is selected with a reduced visibility of 5 km. For all three cases the LOWTRAN aerosol model is employed, with the relative humidity set to 80% in summer and 70% in winter. Background conditions are assumed for the free troposphere, stratosphere and mesosphere.

The viewing geometry of SCIAMACHY allows it to scan to $\pm 30^\circ$ around the nadir line of sight. Unfortunately every model spectrum must be calculated for the exact nadir position, as the computational time for off axis spectra is very high. To account for the increased path-length in off-axis viewing geometry, a correction has been be applied to the final retrieved column (Buchwitz et al., 2000). This is not an ideal solution, as it can cause an over correction of up to 2–3% for pixels at the extremities (Buchwitz and Burrows, 2004). All SCIAMACHY observations are cloud screened prior to retrieval processing, with cloud contaminated pixels flagged and disregarded using the current

version of the Heidelberg Iterative Cloud Retrieval Utilities (HICRU) database (Grzegorski et al., 2005). Where gaps occur in this database or if the HICRU algorithm fails then an alternative method is employed which uses the polarization measurement devices, specifically PMD1, flagging a pixel if a pre-defined threshold (set at 70 000 BU) is exceeded (de Beek et al., 2004). Despite this, it is evident that cloudy pixels are still processed. Such columns are easily noticeable by their extremely low mixing ratios and low correlation with the surface elevation. These are subsequently filtered out after processing. Back-scans along with observations that have solar zenith angles greater than 75° are also excluded. All columns are normalized to the ECMWF surface pressure.

5 Preliminary results

The calculation of a reference spectrum for each SCIAMACHY observation, whilst felt necessary, is still time-consuming at approximately 5 min per ground pixel. This means that, at this stage, FSI-WFM-DOAS can only be applied to selected "target regions" that are of particular scientific interest. In this first demonstration of the FSI algorithm, Siberia has been chosen as an example test region, specifically the area bounded by the latitudes 48° N–80° N and the longitudes of 45° E–180° E, with just the summer months processed (excluding August during which SCIAMACHY underwent a decontamination phase to remove ice on the NIR detectors). To ensure only valid retrievals are examined, only columns that have retrieval errors less than 5% and lie within a quite broad range of 340–400 ppmv are accepted. These results are summarized in Table 4. In this initial analysis, comparisons to chemical transport models, for example the TM3 model (Heimann and Körner, 2003) or ground station data are not made, as this will be the goal of future research. Instead the focus is on the quality of the spectral fits and possible errors and biases associated with the FSI WFM-DOAS retrieval. Hence, in this study neither the retrieved columns (in molecules per cm^2) or the normalized columns (in ppmv), have had scaling factors applied as in other studies (e.g.

Yang et al., 2002 or Buchwitz et al., 2005), thus only the CO_2 spatial distribution can really be discussed.

The spectral fits produced by the FSI algorithm are promising, with a typical fit shown in Fig. 8. The CO_2 fit indicates that there is good sensitivity to the CO_2 vertical column unlike temperature, where the fit is much worse. If the retrievals are repeated but this time only fitting the CO_2 and H_2O weighting functions, then the that magnitude of the vertical columns increases but their relative spatial distribution remains the same. Fitting the temperature derivative therefore only creates a negative offset, suggesting that the current algorithm is more sensitive to other factors, possibly calibration issues. Nevertheless, it is always included, following the sensitivity study presented in Sect. 3. By averaging over all retrievals, the mean fit residual should ideally reflect only measurement noise. However, this is not the case, illustrated by Fig. 9, as it contains quite, stable systematic structures, the origin of which has yet to be clarified. It is most likely that such features will be reduced (or removed) by improving the calibration of the SCIAMACHY spectra and through continually including the latest spectroscopic data in the radiative transfer model. The residuals are also strongly influenced by the slit function used in the convolution of the reference spectra and weighting functions. From close examination of the fit residuals, a Gaussian slit function of width 1.4 nm has been implemented as this yields the lowest retrieval errors and best fits. The root-mean-square (RMS) error, over the time-period considered, is extremely consistent at about 0.2% showing that the FSI algorithm is very stable (Table 4).

Although the algorithm uses several sources of a priori information it is important to ensure that the retrieved columns are not biased from the input data. This is especially relevant with regards to the a priori CO_2 vertical columns, the surface albedo and surface pressure. The a priori and retrieved CO_2 vertical columns for June (Fig. 10) demonstrate that whilst the spatial distribution of input columns is moderately smooth (essentially following the surface topography) the measured columns exhibit much more variation. The correlation between the two sets of columns, though relatively high at 0.82, is acceptable considering the low variability in the total column (Fig. 11).

For the surface albedo no such correlation is found (Fig. 12), although the retrievals errors increase when the surface reflectance becomes progressively lower (i.e. as SCIAMACHYs signal to noise ratio decreases). Concerning the input ECMWF surface pressure, the correlation with the retrieved vertical column densities is again, quite high at 0.82 but is to be somewhat expected with CO_2 being well mixed in the atmosphere. If comparisons are made to the surface elevation (Fig. 13) however, which is on a finer resolution grid, then a slight bias is noticeable in that a significant fraction of the columns lie below the 3% (and indeed 5%) variability associated with the US Standard atmosphere. This in itself, is not indicative that retrieval algorithm produces this bias as it is possible that a large number of these low column densities may still be partially cloud contaminated. Alternatively, these low values maybe a calibration related effect but whatever the origin this systematic underestimation requires further examination. Checks for trends and biases in the retrieved CO_2 columns related to the longitudinal and latitudinal distribution of the ground pixels; the line of sight and solar zenith angles and the a priori and retrieved water vapour columns were also performed. In all circumstances no correlation was found. This analysis was also repeated for the retrieval error associated with CO_2 columns with again, no biases detected.

Having considered the quality of the FSI retrieval algorithm, its results are shown in Fig. 14 with all normalized columns averaged on to a $1^\circ \times 1^\circ$ grid. The most noticeable feature of these monthly fields is the fairly high variability of the CO_2 concentration, with the 1σ deviation about each monthly mean being $\sim$10 ppmv. Whilst some of this variability may be realistic it is probable that some of the deviations maybe removed by normalizing the retrieved CO_2 columns with oxygen (O_2) columns, instead of the surface pressure. By taking the ratio with oxygen, which can also be retrieved from SCIAMACHY, the effects of aerosols and clouds on the light path may cancel out. This so-called dry mixing ratio denoted XCO_2 ($=CO_2/O_2 \times 0.295$) is used to reduce systematic errors in satellite retrievals and is already implemented by Buchwitz et al. (2005) and proposed for the future Orbiting Carbon Observatory (OCO) mission (Crisp et al., 2004). This not withstanding, distinct evolving patterns within the CO_2 distribution are

visible, for example there is an enhanced region over the Yablononvyy mountain range (approximately 115° E 49° N) in May and what seems to be a persistent dip in the CO_2 concentration over the West Siberian Plain in the vicinity of 75° E 60° N. Similarly the seasonal uptake of CO_2 by the biosphere appears to be detectable with a decline in the concentration from May to July before increasing again by September. Whether these features are created by CO_2 surface fluxes is yet unproven and warrants further investigation. Nevertheless it is encouraging that some structure within the CO_2 fields is visible and may possibly provide information on important carbon processes occurring within the Siberian region. As more SCIAMACHY data is processed the identification of CO_2 surface fluxes will be the goal of future research efforts.

6 Conclusions

The ability of the WFM-DOAS retrieval algorithm to measure total columns of atmospheric CO_2 has been closely examined. A detailed sensitivity analysis has been performed that has identified several non-negligible error sources and time dependent biases which affect the accuracy of the retrieved CO_2 columns. These inaccuracies originate from using a reference spectrum which is created from a differing atmospheric state to that of the measurement. To minimize these errors a new CO_2 retrieval algorithm called Full Spectral Initiation (FSI) WFM-DOAS has been developed, the foundation of which is the use of a priori data to obtain the best possible linearization point for the retrieval. The FSI algorithm has then been applied to SCIAMACHY observations with both the quality of the spectral fits and possible biases assessed. Although some of the CO_2 columns appear to be under-estimated there isn't any evidence of a priori influence in the retrieved data. Preliminary results for the summer months over Siberia have shown that the retrieved monthly fields exhibit a significant amount of variability but that some structure in the CO_2 concentration is visible.

Acknowledgements. The authors would like to thank J. Burrows and the team at IUP Bremen for providing such a useful instrument and for supplying preliminary SCIAMACHY data. Many

thanks go to M. Buchwitz and C. Frankenberg for giving very helpful advice and comments. We are also grateful to M. Grzegorski for providing the HICRU cloud data and A. Rozanov for supplying the radiative transfer model SCIATRAN. We would like to thank ESA for supplying the SCIAMACHY data, all of which was processed by DLR, and the British Atmospheric Data Centre (BADC) for supplying the ECMWF operational data set. The authors finally wish to thank both the Natural Environment Research Council (NERC) and CASIX (the Centre for observation of Air-Sea Interactions and fluXes) for supporting M. Barkley through grant ref: NER/S/D/200311751.

References

Anderson, B. E., Gregory, G. L., Collins Jr., J. E., Sachse, G. W., Conway, T. J., and Whiting, G. P.: Airborne observations of spatial and temporal variability of tropospheric carbon dioxide, J. Geophys. Res., 101, 1985–1997, 1996. 2768, 2772

Bovensmann, H., Burrows, J. P., Buchwitz, M., Frerick, J., Nöel, S., Rozanov, V. V., Chance, K. V., and Goede, A.: SCIAMACHY – mission objectives and measurement modes, J. Atmos. Sci., 56, 127–150, 1999. 2769

Buchwitz, M. and Burrows, J. P.: Retrieval of CH_4, CO, and CO_2 total column amounts from SCIAMACHY near-infrared nadir spectra: Retrieval algorithm and first results, in: Remote Sensing of Clouds and the Atmosphere VIII, Proceedings of SPIE, edited by: Schäfer, K. P., Comèron, A., Carleer, M. R., and Picard, R. H., 5235, 375–388, 2004. 2770, 2771, 2773, 2775, 2779

Buchwitz, M., Rozanov, V. V., and Burrows, J. P.: A near infrared optimized DOAS method for the fast global retrieval of atmospheric CH_4, CO, CO_2, H_2O, and N_2O total column amounts from SCIAMACHY/ENVISAT-1 nadir radiances, J. Geophys. Res., 105, 15 231–15 246, 2000. 2766, 2770, 2779

Buchwitz, M., de Beek, R., Bramstedt, K., Nöel, S., Bovensmann, H., and Burrows, J. P.: Global carbon monoxide as retrieved from SCIAMACHY by WFM-DOAS, Atmos. Chem. Phys., 4, 1945–1960, 2004. 2769

Buchwitz, M., de Beek, R., Nöel, S., Burrows, J. P., Bovensmann, H., Bremer, H., Bergamaschi, P., Körner, S., and Heimann, M.: Carbon monoxide, methane and carbon dioxide columns

retrieved from SCIAMACHY by WFM-DOAS: year 2003 initial data set, Atmos. Chem. Phys., 5, 3313–3329, 2005. 2769, 2776, 2781, 2782

Chédin, A., Saunders, R., Hollingsworth, A., Scott, N. A., Matricardi, M., Etcheto, J., Clerbaux, C., Armante, R., and Crevoisier, C.: The feasibility of monitoring CO_2 from high-resolution infrared sounders, J. Geophys. Res., 108, 4064, doi:10.1029/2001JD001443, 2003. 2768

Ciais, P., Tans, P. P., Trollier, M., White, J. W., and Francey, R. J.: A large Northern Hemisphere terrestrial CO_2 sink indicated by the $^{13}C/^{12}C$ ratio of atmospheric CO_2, Science, 269, 1098–1101, 1995. 2767

Conway, T. J., Tans, P. P., Waterman, L. S., Thoning, K. W., Kitzis, D. R., Masarie, K. A., and Zhang, N.: Evidence for interannual variability of the carbon cycle from the National Oceanic and Atmospheric Administration/Climate Monitoring and Diagnostic Laboratory Global Air Sampling, J. Geophys. Res., 99, 22 831–22 855, 1994. 2768

Crisp, D., Atlas, R., Bréon, F.-M., Brown, L., Burrows, J., Ciais, P.and Connor, B., Doney, S., Fung, I., Jacob, D., Miller, C., O'Brien, D., Pawson, S., Randerson, J., Rayner, P., Salawitch, R., Sander, S., Sen, B., Stephens, G., Tans, P., Toon, G., Wennberg, P., Wofsy, S., Yung, Y., Kuang, Z., Chudasama, B., Sprague, G., Wiess, B., Pollock, R., Kenyon, D., and Schroll, S.: The Orbiting Carbon Observatory (OCO) mission, Adv. Space Res., 34(4), 700–709, 2004. 2782

de Beek, R., Gloudemans, A., Schrijver, H., Frankenberg, C., Grzegorski, M., Wagner, T., and Buchwitz, M.: Retrieval algorithm development for EVERGREEN using SCIAMACHY: Status and analyses for optimization, Technical Note (EU Contract EVG1-CT-2002-00079),TN-EVG-TASK1-RET-001, 2004. 2780

Dufour, E. and Bréon, F.: Spaceborne estimate of atmospheric CO_2 column by use of the differential absorption method: error analysis, Appl. Opt., 42, 3595–3609, 2003. 2768, 2775, 2776

Frankenberg, C., Meirink, J. F., van Weele, M., Platt, U., and Wagner, T.: Assessing Methane Emissions from Global Space-Borne Observations, Science, 308, 1010–1014, 2005a. 2769

Frankenberg, C., Platt, U., and Wagner, T.: Retrieval of CO from SCIAMACHY onboard ENVISAT: detection of strongly polluted areas and seasonal patterns in global CO abundances, Atmos. Chem. Phys., 5, 1639–1644, 2005b. 2769, 2778

Frankenberg, C., Platt, U., and Wagner, T.: Iterative maximum a posteriori (IMAP)-DOAS for retrieval of strongly absorbing trace gases: Model studies for CH_4 and CO_2 retrieval from near infrared spectra of SCIAMACHY onboard ENVISAT, Atmos. Chem. Phys., 5, 9–22,

2005c. 2775, 2777
GLOBALVIEW-CO_2: Cooperative Atmospheric Data Integration Project – Carbon Dioxide, CD-ROM, NOAA CMDL, Boulder, Colorado [Also available on Internet via anonymous FTP to ftp://ftp.cmdl.noaa.gov, Path:ccg/co2/GLOBALVIEW], 2005. 2767
Gloudemans, A. M. S., Schrijver, H., Kleipool, Q., van den Broek, M. M. P., Straume, A. G., Lichtenberg, G., van Hees, R., Aben, I., and Meirink, J. F.: The impact of SCIAMACHY near-infrared instrument calibration on CH_4 and CO total columns, Atmos. Chem. Phys., 5, 2369–2383, 2005. 2778
Grzegorski, M., Frankenberg, C., Platt, U., Sangahvi, S., Fournier, N., Stammes, P., and Wagner, T.: Application of the HICRU cloud algorithm on SCIAMACHY: design and intercomparision, Geophys. Res. Abstr., 7, 08 316, 2005. 2780
Gurney, K. R., Law, R. M., Denning, A. S., Rayner, P. J., Baker, D., Bousquet, P., Bruhwilerk, L., Chen, Y.-H., Ciais, P., Fan, S., Fung, I. Y., Gloor, M., Heimann, M., Higuchi, K., John, J., Maki, T., Maksyutov, S., Masariek, K., Peylin, P., Pratherkk, M., Pakkk, B. C., Randerson, J., Sarmiento, J., Taguchi, S., Takahashi, T., and Yuen, C.-W.: Towards robust regional estimates of sources and sinks using atmospheric transport models, Nature, 415, 626–630, 2002. 2767
Heimann, M. and Körner, S.: The Global Atmospheric Tracer Model TM3, Model Description and Users Manual Release 3.8a, Tech. Rep. 5, Max Planck Institute for Biogeochemistry (MPI-BGC), Jena, Germany, 2003. 2780
Hess, M., Koepke, P., and Schult, I.: Optical properties of aerosols and clouds: The software package OPAC, Bull. Amer. Meteorol. Soc., 75, 831–844, 1998. 2776
Holzer-Popp, T., Schroedter, M., and Gesell, G.: Retrieving aerosol optical depth and type in the boundary layer over land and ocean from simultaneous GOME spectrometer and ATSR-2 radiometer measurements, 1. Method description, J. Geophys. Res., 107, 4578, doi:10.1029/2001JD002 013, 2002. 2792
Hoogen, R.: Aerosol Parameterization in GOMETRAN ++, Institt fur Umweltphysik, Universtät Bremen, Internal report, 1995. 2776
Houweling, S., Hartmann, W., Aben, I., Schrijver, H., Skidmore, J., Roelofs, G.-J., and Brëon, F.-M.: Evidence of systematic errors in SCIAMACHY-observed CO_2 due to aerosols, Atmos. Chem. Phys., 5, 3003–3013, 2005. 2769, 2776
Intergovernmental Panel on Climate Change: Climate Change 2001: Synthesis Report: Third Assessment Report of the Intergovernmental Panel on Climate Change, Cambridge Univer-

sity Press, New York, 2001. 2767
Kawa, S. R., Erickson-III, D. J., Pawson, S., and Zhu, Z.: Global CO_2 transport simulations using meteorological data from the NASA data assimilation system, J. Geophys. Res., 109, D18 312, doi:10.1029/2004JD004554, 2004. 2775
Kleipool, Q.: Algorithm Specification for Dark Signal Determination, Tech. rep., SRON-SCIA-30 PhE-RP-009, SRON, 2003a. 2778
Kleipool, Q.: Recalculation of OPTEC5 Non-Linearity, Report containing the NL correction to be implemented in the data processor, Tech. rep. SRON-SCIA-PhE-RP-013, SRON, 2003b. 2778
Kleipool, Q.: SCIAMACHY: Evolution of Dead and Bad Pixel Mask, Tech. Report SRON-SCIA-PhE-RP-21, SRON, 2004. 2778
Kneizys, F. X., Shettle, E. P., Abreu, L. W., Chetwynd, J. H., Anderson, G. P., Gallery, W. O., Selby, J. E. A., and Clough, S. A.: A users guide to LOWTRAN 7, Tech. rep. Air Force Geophysics Laboratory AFGL, 1986. 2771
Kneizys, F. X., Abreu, L. W., Anderson, G. P., Shettle, E. P., Chetwynd, J. H., Shettle, E. P., Berk, A., Bernstein, L., Robertson, D., Acharya, P., Rothman, L., Selby, J. E. A., Allery, W. O., and Clough, S. A.: The MODTRAN 2/3 report and LOWTRAN 7 model, Tech. rep., Philips Laboratory, Hanscom AFB, 1996. 2771, 2776
Kuang, Z., Margolis, J., Toon, G., Crisp, D., and Yung, Y.: Spaceborne measurements of atmospheric CO_2 by high-resolution NIR spectrometry of reflected sunlight: An introductory study, Geophys. Res. Lett., 29, 1716, doi:10.1029/2001GL014298, 2002. 2768
Kuck, L. R., Smith Jr., T. S., Balsley, B. B., Helmig, T., Conway, T. J., Tans, P. P., Davis, K., Jensen, M. L., Bognar, J. A., Vazquez Arrieta, R., Rodriquez, R., and Birks, J. W.: Measurements of landscape fluxes of carbon dioxide in the Peruvian Amazon by vertical profiling through the atmospheric boundary layer, J. Geophys. Res., 105, 22 137–22 146, 2000. 2768
Levin, I., Ciais, P., Langenfelds, R., Schmidt, M., Ramonet, M., Sidorov, K., Tchebakova, N., Gloor, M., Heimann, M., Schulze, E., Vygodskaya, N., Shibistova, O., and Lloyd, J.: Three years of trace gas observations over the EuroSiberian domain derived from aircraft sampling – a concerted action, Tellus, 54B, 696–712, 2002. 2768
Lichtenberg, G. , Kleipool, Q., Krijger, J. M., van Soest, G., van Hees, R., Tilstra, L. G., Acarreta, J. R., Aben, I., Ahlers, B., Bovensmann, H., Chance, K., Gloudemans, A. M. S., Hoogeveen, R. W. M., Jongma, R., Nol, S., Piters, A., Schrijver, H., Schrijvers, C., Sioris, C. E., Skupin, J., Slijkhuis, S., Stammes, P., and Wuttke, M.: SCIAMACHY Level1 data: Calibration concept

and in-flight calibration, Atmos. Chem. Phys. Discuss., 5, 8925–8977, 2005. 2778
Mao, J. and Kawa, S. R.: Sensitivity studies for space-based measurement of atmospheric measurement of atmospheric total column carbon dioxide by reflected sunlight, Appl. Opt., 43, 914–927, 2004. 2768
Matsueda, H., Inoue, H. Y., and Ishii, M.: Aircraft observations of carbon dioxide at 8–13 km altitude over the western Pacififc from 1933 to 1999, Tellus, 54B, 1–21, 2002. 2768
McClatchey, R. A., Fenn, R. W., Selby, J. E. A., Volz, F. E., and Garing, J. S.: Optical properties of the atmosphere, 3rd ed., Environ. Res. Pap. 411, AFCRL-72-0497, Air Force Cambridge Res. Lab., Bedford, Mass., 1972. 2771, 2773
Nakazawa, T., Miyashita, K., Aoki, S., and Tanaka, M.: Temporal and spatial variations of upper tropospheric and lower stratospheric carbon dioxide, Tellus, 43B, 106–117, 1991. 2768
Nakazawa, T., Murayama, S., Miyashita, K., Aoki, S., and Tanaka, M.: Longitudinally different variations of lower tropospheric carbon dioxide concentrations over the North Pacific Ocean, Tellus, 44B, 161–172, 1992. 2768
Nakazawa, T., Sugawara, S., Inoue, G., Machida, T., Makshyutov, S., and Mukai, H.: Aircraft measurements of the concentrations of CO_2, CH_4, N_2O and CO in the troposphere over Russia, J. Geophys. Res., 102, 3843–3859, 1997. 2768, 2772
O'Brien, D. M. and Rayner, P. J.: Global observations of the carbon budget, 2. CO_2 column from differential absorption of reflected sunlight in the 1.61μm band of CO_2, J. Geophys. Res., 107(D18), 4354, doi:10.1029/2001JD000617, 2002. 2768
Olsen, S. C. and Randerson, J. T.: Differences between surface and column atmospheric CO_2 and implications for carbon cycle research, J. Geophys. Res., 109, D02 301, doi:10.1029/2003JD003968, 2004. 2768
Rayner, P. J. and O'Brien, D. M.: The utility of remotely sensed CO_2 concetration data in surface source inversions, Geophys. Res. Lett., 28, 175–178, 2001. 2768
Rödenbeck, C., Houweling, S., Gloor, M., and Heimann, M.: CO_2 flux history 1982-2001 inferred from atmospheric data using a global inversion of atmospheric transport, Atmos. Chem. Phys., 3, 1919–1964, 2003. 2767
Rothman, L., Jacquemart, D., Barbe, A., Benner, C. D., Birk, M., Brown, L. R., Carleer, M. R., Chackerian Jr., C., Chance, K., Coudert, L. H., Dana, V., Devi, V. M., Flaud, J.-M., Gamache, R. R., Goldman, A., Hartmann, J.-M., Jucks, J. W., Maki, A. G., Mandin, J.-Y., Massie, S. T., Orphal, J., Perrin, A., Rinsland, C. P., Smith, M., Tennyson, J., Tolchenov, R. N., Toth, R. A., Vander Auwera, J., Varanasi, P., and Wagner, G.: The *HITRAN* 2004 molecular

spectroscopic database, J. Quant. Spectrosc. Radiat. Transfer, 96, 193–204, 2005. 2779
Rozanov, V. V., Buchwitz, M., Eichmann, K. U., de Beek, R., and Burrows, J. P.: SCIATRAN – a new radiative transfer model for geophysical applications in the 240–2400 nm spectral region: The pseudo-spherical version, presented at COSPAR 2000, Adv. Space Res., 29(11), 1831–1835, 2002. 2771
Sidorov, K., Sogachev, A., Langendörfer, U., Lloyd, J., Nepomniachii, I. L., Vygodskaya, N. N., Schmidt, M., and Levin, I.: Seasonal variability of greenhouse gases in the lower troposphere above the eastern European taiga (Syktyvkar, Russia), Tellus, 54B, 735–748, 2002. 2768
Tans, P. P., Fung, I. Y., and Takahashi, T.: Observational constraints on the global atmospheric CO_2 budget, Science, 247, 1431–1438, 1990. 2767
Vay, S., Anderson, B. E., Conway, T. J., Collins Jr., J. E., Blake, D. R., and Westberg, D. J.: Airborne observations of tropospheric CO_2 distribution and its controlling factors over the South Pacific Basin, J. Geophys. Res., 101, 1985–1997, 1999. 2768
Yang, Z. H., Toon, G. C., Margolis, J. S., and Wennberg, P. O.: Ground based inversion of CO_2 column densities from solar spectra, Geophys. Res. Lett., 29, doi:10.1029/2001GL014537, 2002. 2781

Table 1. Relative errors produced in the retrieved CO_2 column created from using alternative temperature and water vapour profiles. Scaling factors of 0.95, 0.97, 1.0, 1.03 and 1.05 applied to the CO_2 column yield mixing ratios of 351.5 ppmv, 358.9 ppmv, 370 ppmv, 381.1 ppmv and 388.5 ppmv respectively. No TWF: temperature weighting function not fitted. TWF: temperature weighting function fitted.

Climatology	Water vapour Scaling	Relative column error (%) CO_2 Column scaling									
		0.95		0.97		1.00		1.03		1.05	
		No TWF	TWF	No TWF	TWF	No TWF	TWF	No TWF	TWF	No TWF	TWF
Tropical	0.5	−2.72	−0.29	−2.68	−0.26	−2.66	−0.25	−2.68	−0.28	−2.71	−0.32
	1.0	−2.78	−0.32	−2.73	−0.29	−2.70	−0.28	−2.71	−0.30	−2.74	−0.34
	1.5	−3.03	−0.46	−2.98	−0.42	−2.94	−0.40	−2.94	−04.2	−2.96	−0.45
Mid Lat Summer	0.5	−3.17	−0.82	−3.00	−0.67	−2.79	−0.49	−2.64	−0.37	−2.56	−0.32
	1.0	−3.20	−0.84	−3.02	−06.9	−2.81	−0.51	−2.65	−0.39	−2.57	−0.33
	1.5	−3.35	−0.94	−3.17	−0.78	−2.94	−0.60	−2.78	−0.47	−2.70	−0.40
Mid Lat Winter	0.5	1.69	−0.04	1.86	0.12	2.06	0.31	2.20	0.45	2.26	0.52
	1.0	1.68	−0.05	1.85	0.11	2.05	0.31	2.19	0.45	2.26	0.51
	1.5	1.66	−0.06	1.83	0.11	2.03	0.30	2.17	0.44	2.24	0.51
Sub Arc Summer	0.5	−1.57	−0.54	−1.40	−0.39	−1.18	−0.20	−1.03	−0.07	−0.95	−0.01
	1.0	−0.02	−0.57	−1.42	−0.41	−1.20	−0.22	−1.04	−0.08	−0.96	−0.02
	1.5	−1.70	−0.63	−1.51	−0.47	−1.29	−0.28	−1.12	−0.13	−1.04	−0.07
Sub Arc Winter	0.5	3.74	−0.31	3.91	−0.13	4.11	0.08	4.26	0.23	4.33	0.32
	1.0	3.73	−0.31	3.90	−0.13	4.11	0.08	4.25	0.24	4.32	0.32
	1.5	3.72	−0.31	3.89	−0.13	4.10	0.08	4.26	0.24	4.32	0.32

Table 2. The error produced in the retrieved CO_2 column brought about from using ECMWF temperature and water vapour profiles instead of the U.S. Standard atmosphere. Each ECMWF profile number corresponds to the indexing in Fig. 3.

	Relative column error %	
ECMWF profile	No TW	TW
1	1.04	−0.70
2	1.01	−1.50
3	3.31	0.90
4	3.86	1.17
5	4.87	−0.89
6	5.26	−0.48
7	−3.99	−1.24
8	2.35	0.94
9	−4.04	−1.29
10	−4.00	−1.31
11	−3.96	−1.24
12	−2.57	−0.39
13	−2.43	−0.32
14	−2.66	−0.41
15	−2.72	−0.24
16	−2.74	−0.25

Table 3. Aerosol error analysis. Inc. Aerosols = Simulated retrievals performed using a reference spectrum with the default aerosol scenario. Exc. Aerosols = Simulated retrievals performed using a reference spectrum without any aerosols present. The component contributions are defined as: waso = watersoluble, inso = insoluble, ssam = sea salt accumulation mode, sscm = sea salt coarse mode, mnuc = mineral nucleation mode, macc = mineral accumulation mode. The biomass burning scenarios were taken from Holzer-Popp et al. (2002). The extinction coefficients within the planetary boundary layer (0–2 km) for the urban smog and biomass burning I & II scenarios were 19.49 km^{-1}, 1.50 km^{-1} and 4.00 km^{-1}.

Aerosol Scenario	Relative Column Error %				Comments
	Inc. aerosols		Exc. aerosols		
	No TWF	TWF	No TWF	TWF	
Continental Clean Summer	1.78	1.88	3.51	3.69	Remote Continental Areas
Continental Clean Winter	0.98	1.04	2.70	2.85	(waso: 99.998%; inso: 0.002%)
Continental Average Summer	1.04	1.11	2.76	2.92	Anthropogenically influenced continental areas
Continental Average Winter	0.22	0.26	1.94	2.06	(waso: 45.79%; inso: 0.01%; soot: 54.20%)
Urban Polluted Summer	−0.44	−0.45	1.27	1.35	Polluted urban areas
Urban Polluted Winter	−4.07	−4.17	−2.39	−2.41	(waso: 31.39%; inso: 0.01%; soot: 68.6%)
Urban Smog Summer	−32.42	−32.84	−31.13	−31.04	Highly polluted urban areas
Urban Smog Winter	−32.49	−32.80	−31.03	−31.34	(waso: 31.39%; inso: 0.01%; soot: 68.6%)
Desert Summer	1.63	1.72	3.36	3.36	Desert regions (e.g. Sahara, Gobi)
Desert Winter	1.27	1.35	3.00	3.15	(mnuc: 93.19%; macc: 6.81%)
Clean Maritime Summer	1.47	1.54	3.20	3.35	Remote marine conditions
Clean Maritime Winter	1.05	1.12	2.78	2.92	(waso: 98.68%; ssam: 1.32%)
Polluted Maritime Summer	1.38	1.45	3.10	3.26	Maritime region under anthropogenic influence
Polluted Maritime Winter	0.65	0.70	2.38	2.51	(waso: 39.4%; ssac: 0.02%; sscm: 0.03%; soot: 60.4%)
Biomass Burning Summer I	−4.06	−4.15	−2.38	3.35	Regions affected by wild fires
Biomass Burning Winter I	−4.05	−4.14	−2.37	−2.38	(waso: 82.00%; inso: 0.01%; soot: 16.60%)
Biomass Burning Summer II	−15.82	−16.30	−14.23	−14.23	Regions affected by heavy biomass burning
Biomass Burning Winter II	−16.09	−16.56	−14.49	−14.92	(waso: 54.00%; inso: 2.00%; soot: 44.00%)

Table 4. Summary of FSI WFM-DOAS retrieval results for the Siberian test region (see Fig. 14) during the summer of 2003.

Month	Number of pixels	Mean CO_2 VMR [ppmv]	1σ VMR [ppmv]	Mean retrieval Error [%]	Mean RMS Error [%]
May	13 612	371.24	11.34	2.52	0.22
June	15 888	365.12	10.10	2.46	0.23
July	21 399	362.15	9.72	2.46	0.24
Sep	24 022	365.15	10.56	2.41	0.27

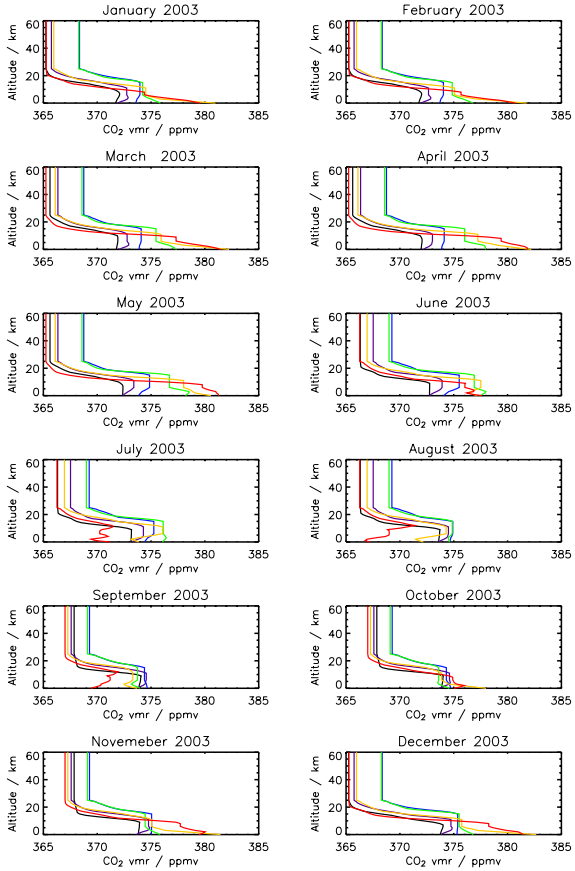

Fig. 1. Vertical CO_2 profiles used in the sensitivity analysis. This data set, for 2003, contains a total of 72 CO_2 profiles, constructed from the flask measurements made by the GLOBALVIEW network. Each month has six profiles centered on the latitudes 75° N (red), 45° N (yellow), 10° N (green), 10° S (blue), 45° S (purple) and 75° S (black), each representative of a 30° latitude band.

ACPD
6, 2765–2807, 2006

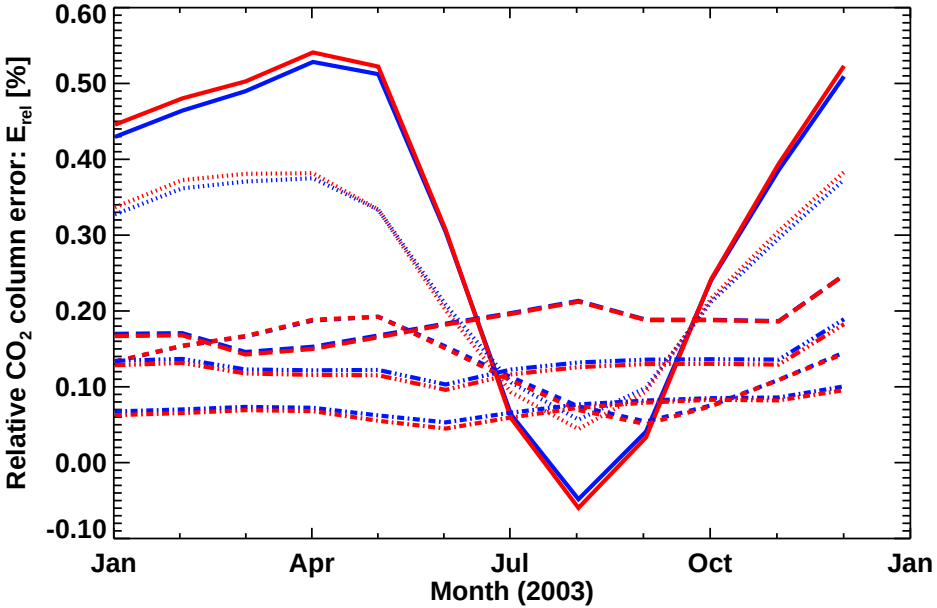

Fig. 2. The relative errors in the retrieved CO_2 column for 75° N (solid), 45° N (dotted), 10° N (dashed), 10° S (dash dot), 45° S (dash dot dot) and 75° S (long dashes) produced by using CO_2 profiles other than the US Standard atmosphere (associated with the reference spectrum), with the simulated retrievals performed both with (red) and without (blue) the temperature weighting function.

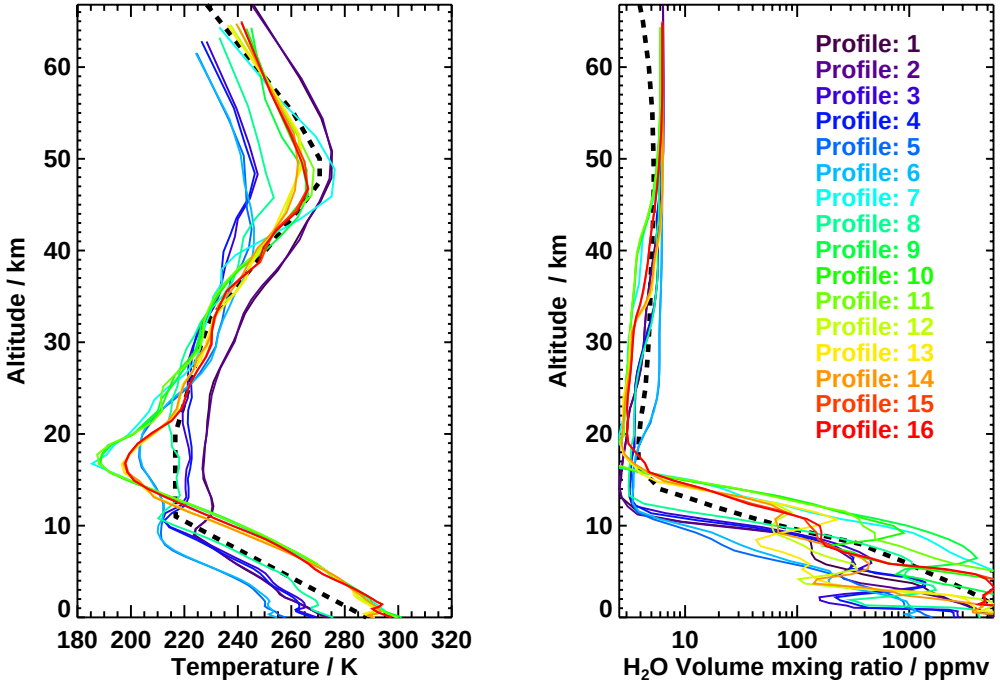

Fig. 3. The ECMWF temperature profiles (left) and corresponding water vapour profiles (right) used in the sensitivity analysis, together with the US standard atmosphere (black dashed line).

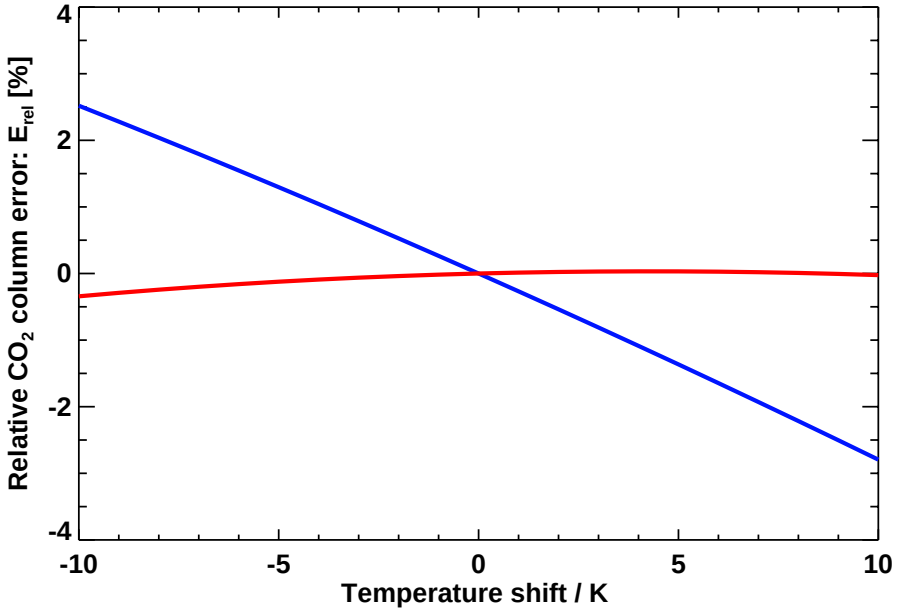

Fig. 4. The sensitivity of the WFM-DOAS algorithm to the temperature linearization point, shown here as a temperature shift of the US Standard Atmosphere, for simulations performed both with/without (red/blue) the temperature weighting function.

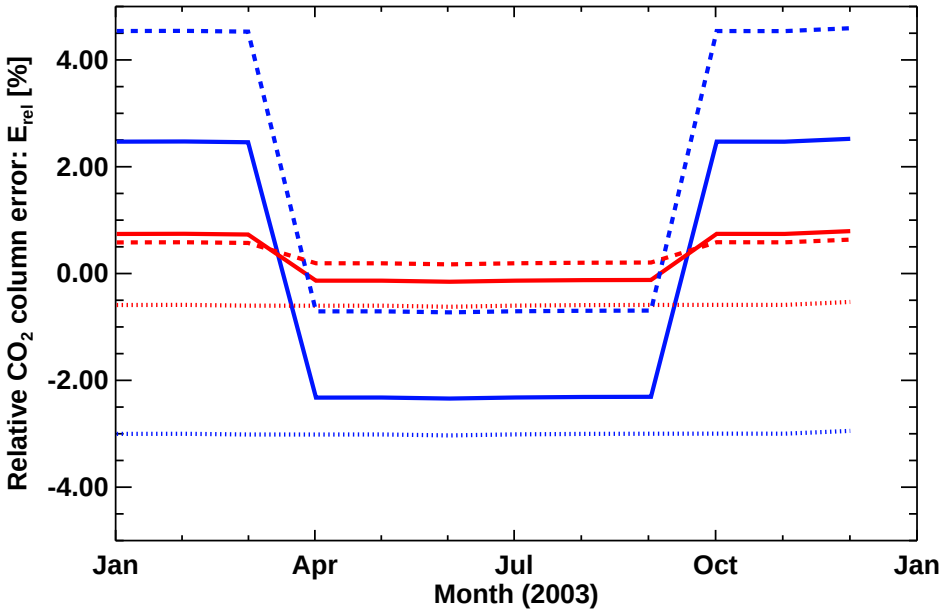

Fig. 5. The relative column error produced by using realistic monthly CO_2 profiles and temperature and water vapour profiles representative of the Northern Hemisphere tropics (dotted), mid-latitudes (solid) and sub-arctic (dashed), for simulated retrievals performed both with/without (red/blue) the temperature weighting function.

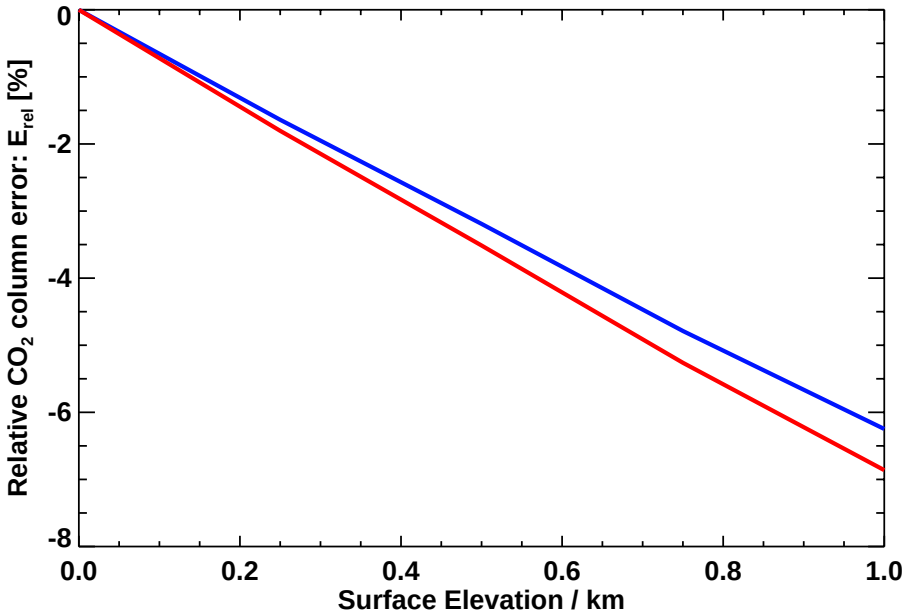

Fig. 6. The relative column error produced as a function of the surface elevation, for simulations performed both with/without (red/blue) the temperature weighting function.. Here the retrieved CO_2 column is systematically under-estimated.

ACPD
6, 2765–2807, 2006

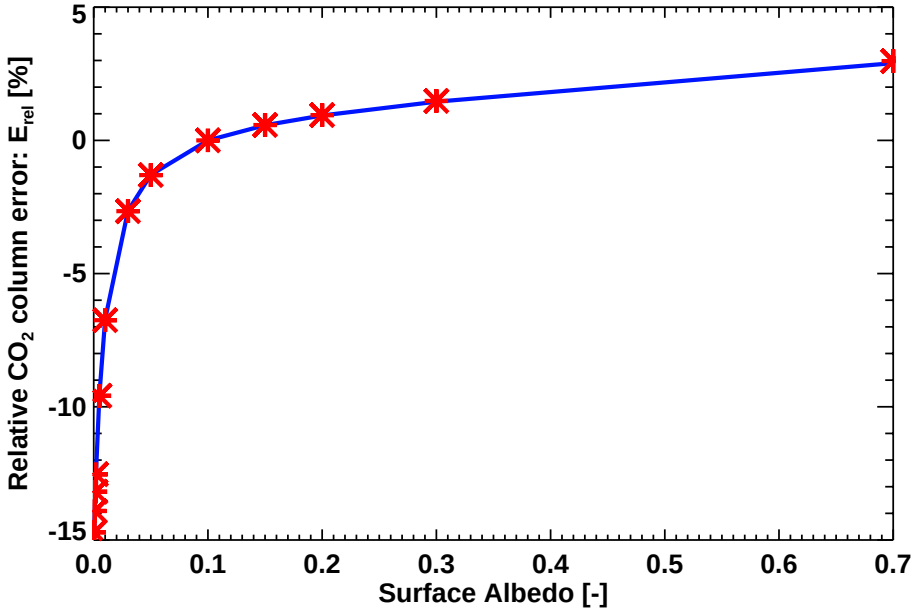

Fig. 7. The relative column error produced as a function of the surface albedo. In this instance the errors produced by fitting (red) and not fitting (blue) the temperature weighting function are barely discernible.

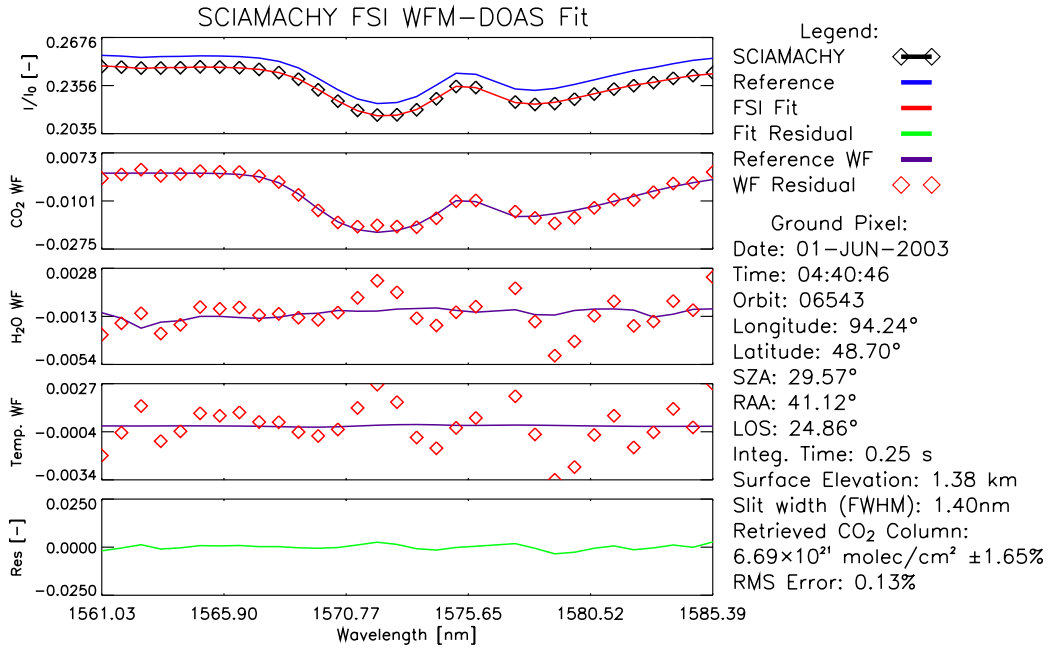

Fig. 8. A typical example of a FSI WFM-DOAS fit. Top panel: The reference spectrum (blue) generated by the retrieval (from the a priori data), the sun-normalized radiance measured by SCIAMACHY (black diamonds) and the FSI WFM-DOAS fit (red) to this measurement. Following three panels: **(i)** The CO_2 fit. This shows CO_2 total column weighting function (WF) scaled by $(\hat{V}_{CO_2} - \bar{V}_{CO_2})$ (purple) and the CO_2 fit residuum (red diamonds), which is the scaled CO_2 WF plus the difference between the measurement and fit (i.e. the fit residual) **(ii–iii)** Similar but for H_2O and temperature. Bottom panel: The fit residual with a root-mean-square (RMS) difference of 0.13%.

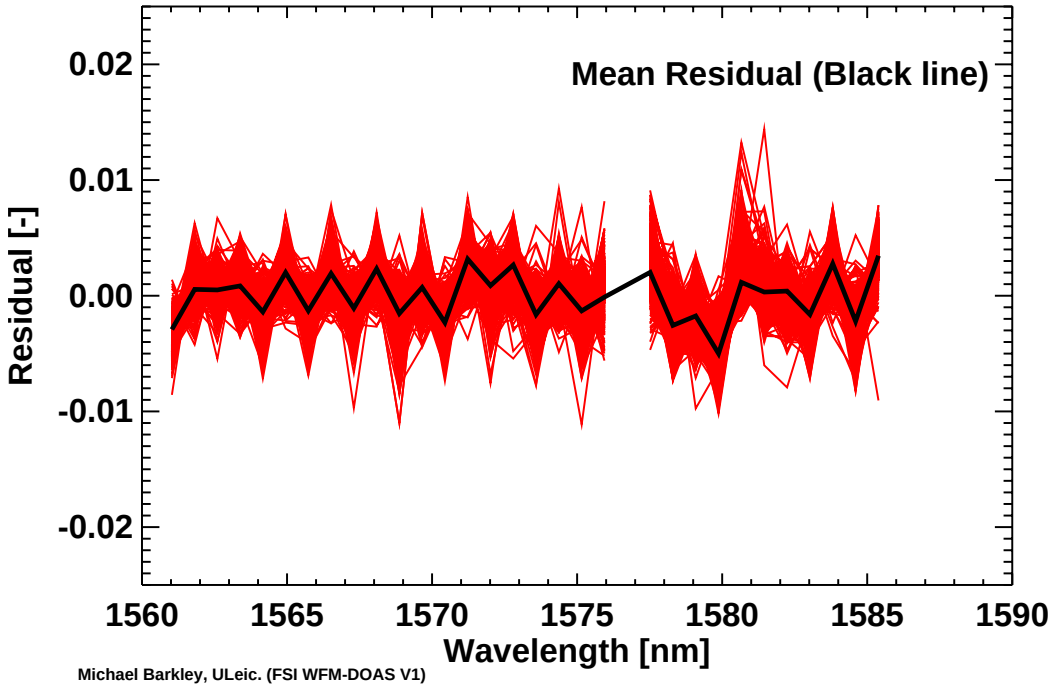

Fig. 9. FSI WFM-DOAS fit residuals for the Siberian test region during May 2003, over-plotted with the mean fit residual (black). The mean RMS error is 0.22%. The detector pixel, of wavelength 1576.72 nm, is omitted in the retrieval as this always worsens the quality of the fit and increases the error on the retrieved column.

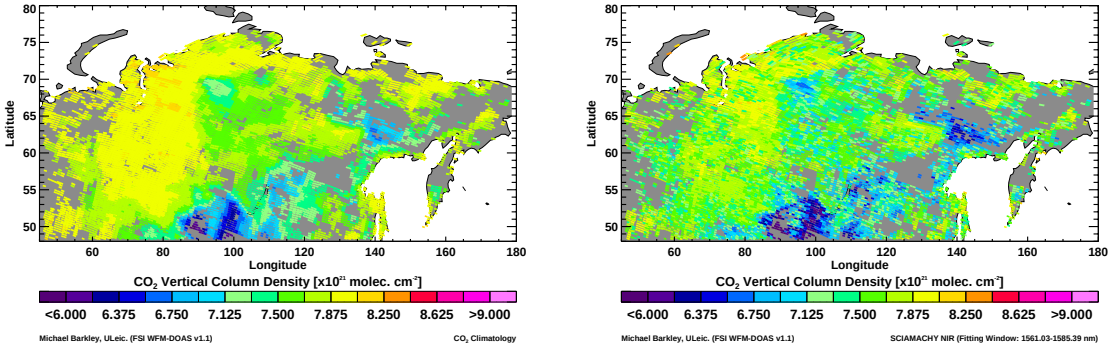

Fig. 10. Left panel: a priori CO_2 columns used in the retrieval for June, 2003, constructed from the CO_2 climatology. Right panel: The FSI WFM-DOAS retrieved CO_2 columns for the same month.

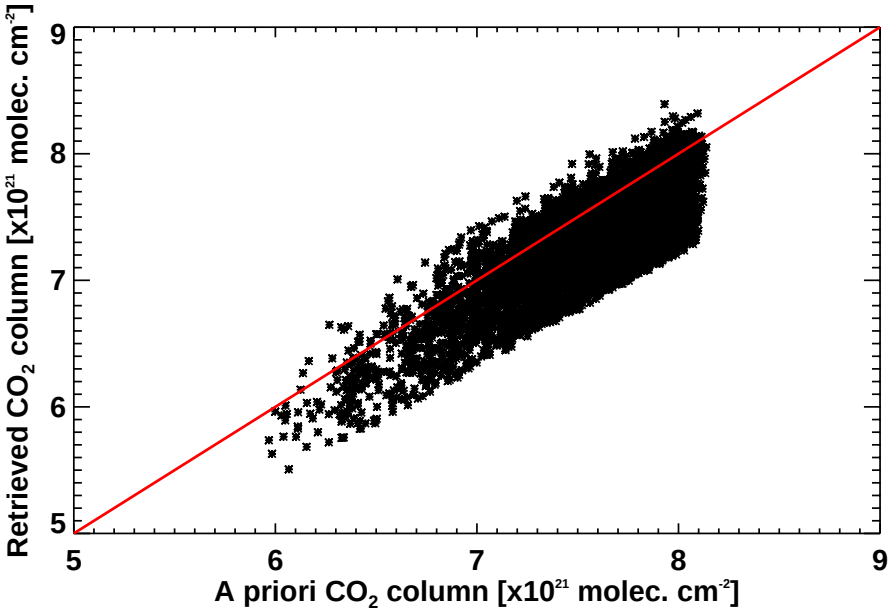

Fig. 11. The retrieved CO_2 columns as a function of the a priori CO_2 columns (shown in Fig. 10) for June 2003. The red line indicates a one-to-one relationship. The linear correlation coefficient between the data is 0.82.

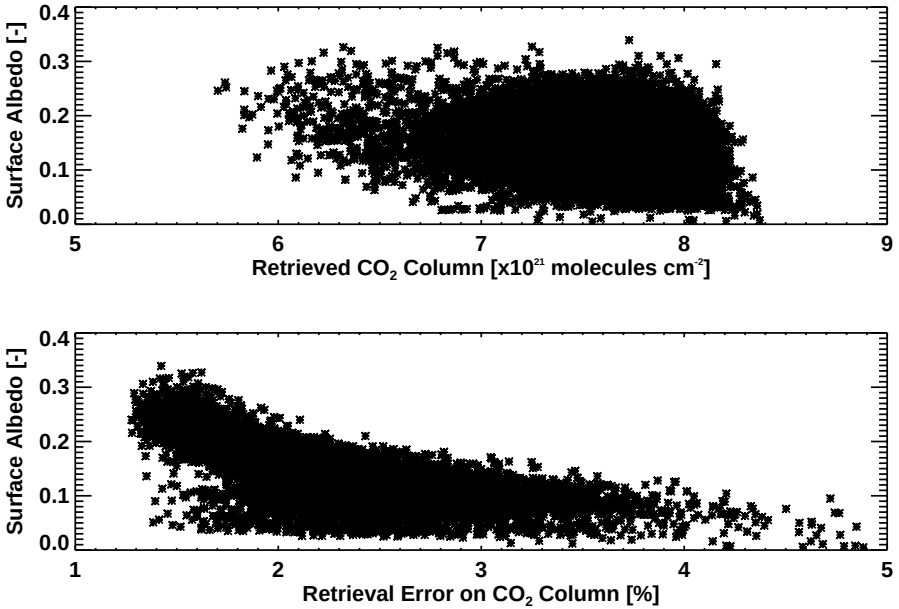

Fig. 12. Top panel: The retrieved CO_2 columns, shown here for the month of May, haven't any dependency on the a priori surface albedo. Bottom panel: The retrieval errors clearly increase when the a priori surface reflectance is small.

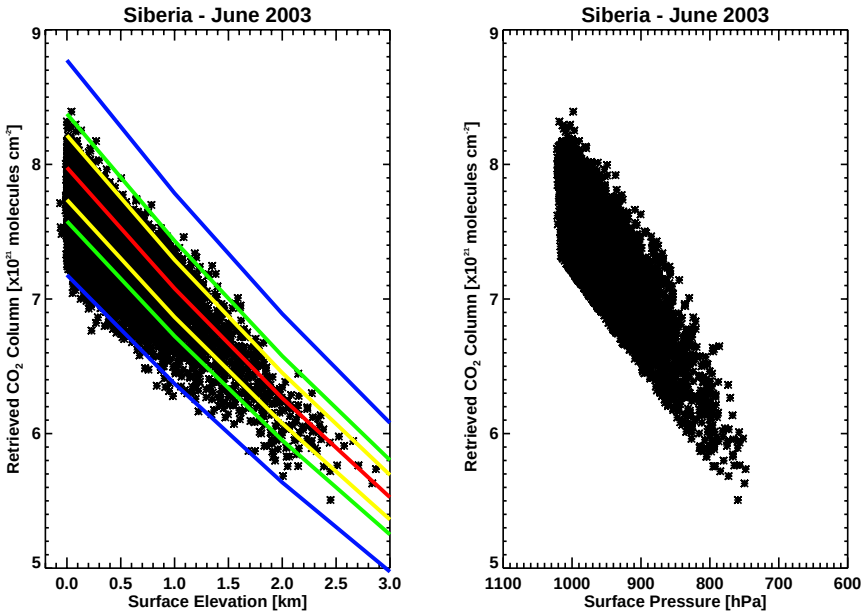

Fig. 13. Left: Comparison between the surface elevation and the retrieved CO_2 columns. The surface elevation is taken from the GLOBE Digital Elevation Model (DEM) (http://www.ngdc.noaa.gov/mgg/topo/globe.html) and averaged to a 0.25°×0.25° grid. The linear correlation coefficient is −0.815. Over-plotted are the variations, of the vertical column density with surface elevation, for the US Standard atmosphere (red), the US Standard atmosphere ±3% variability in the total column (yellow), the US Standard atmosphere ±5% variability (green) and the US Standard atmosphere ±10% variability (blue). Right: The variation of the retrieved CO_2 column with the a priori ECMWF surface pressure, which has a correlation coefficient of 0.82.

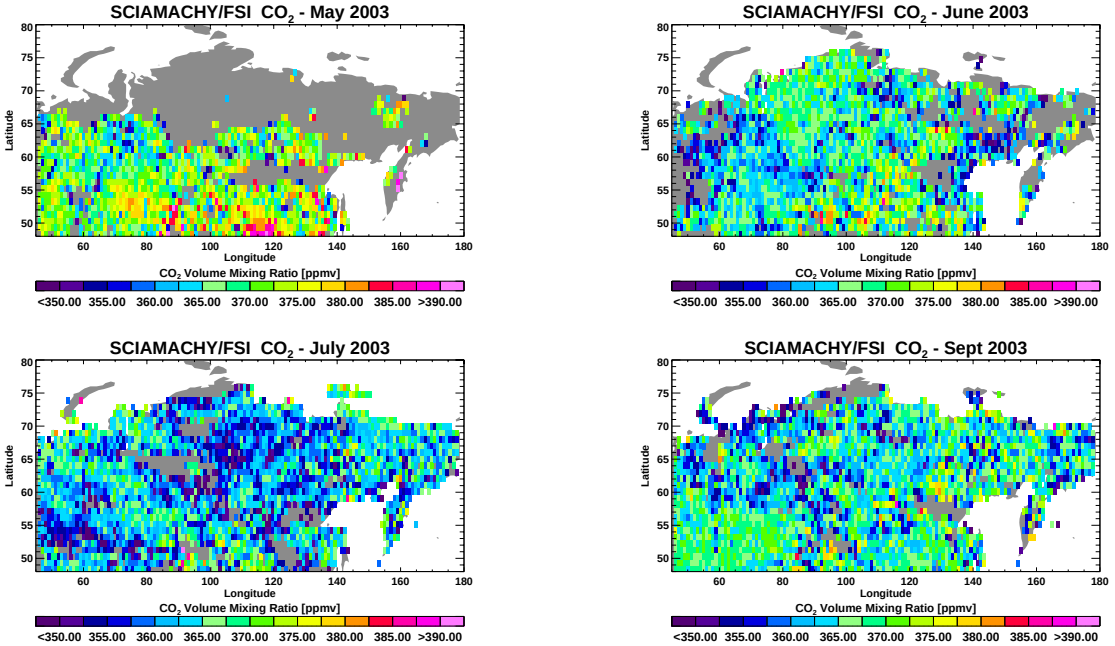

Fig. 14. Normalized CO_2 columns, retrieved over the Siberian test region for the summer of 2003, averaged on to a $1^\circ \times 1^\circ$ grid.

ACPD
6, 2765–2807, 2006